



Lawrence Berkeley Laboratory

UNIVERSITY OF CALIFORNIA

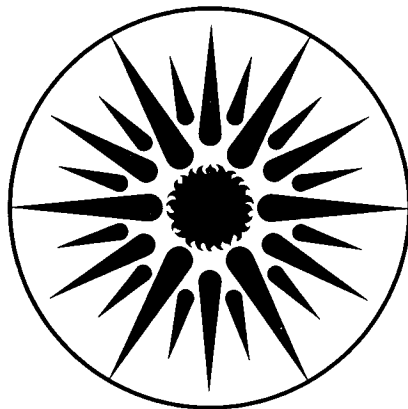
ENERGY & ENVIRONMENT DIVISION

Submitted to Health Physics

Modeling Radon Entry into Florida Slab-on-Grade Houses

K.L. Revzan, W.J. Fisk, and R.G. Sextro

August 1992



ENERGY & ENVIRONMENT
DIVISION

1 LOAN COPY 1
1 Circulates 1
1 for 4 weeks 1 Bldg. 50 Library.
Copy 2

LBL-32472

DISCLAIMER

This document was prepared as an account of work sponsored by the United States Government. Neither the United States Government nor any agency thereof, nor The Regents of the University of California, nor any of their employees, makes any warranty, express or implied, or assumes any legal liability or responsibility for the accuracy, completeness, or usefulness of any information, apparatus, product, or process disclosed, or represents that its use would not infringe privately owned rights. Reference herein to any specific commercial product, process, or service by its trade name, trademark, manufacturer, or otherwise, does not necessarily constitute or imply its endorsement, recommendation, or favoring by the United States Government or any agency thereof, or The Regents of the University of California. The views and opinions of authors expressed herein do not necessarily state or reflect those of the United States Government or any agency thereof or The Regents of the University of California and shall not be used for advertising or product endorsement purposes.

Lawrence Berkeley Laboratory is an equal opportunity employer.

DISCLAIMER

This document was prepared as an account of work sponsored by the United States Government. While this document is believed to contain correct information, neither the United States Government nor any agency thereof, nor the Regents of the University of California, nor any of their employees, makes any warranty, express or implied, or assumes any legal responsibility for the accuracy, completeness, or usefulness of any information, apparatus, product, or process disclosed, or represents that its use would not infringe privately owned rights. Reference herein to any specific commercial product, process, or service by its trade name, trademark, manufacturer, or otherwise, does not necessarily constitute or imply its endorsement, recommendation, or favoring by the United States Government or any agency thereof, or the Regents of the University of California. The views and opinions of authors expressed herein do not necessarily state or reflect those of the United States Government or any agency thereof or the Regents of the University of California.

MODELING RADON ENTRY INTO FLORIDA SLAB-ON-GRADE HOUSES

K.L. Revzan, W.J. Fisk, R.G. Sextro
Indoor Environment Program
Applied Science Division
Lawrence Berkeley Laboratory
1 Cyclotron Road
Berkeley, CA 94720

August, 1992

This work was supported by the U.S. Environmental Protection Agency (EPA) through Interagency Agreement DW89934620-0 with the U.S. Department of Energy (DOE). This work was also supported by the Assistant Secretary for Conservation and Renewable Energy, Office of Building Technologies, Building Systems and Materials Division and by the Director, Office of Energy Research, Office of Health and Environmental Research of DOE under contract DE-AC03-76SF00098.

Abstract

We model radon entry into a Florida house whose concrete slab is supported by a permeable concrete-block stem wall and a concrete footer. The slab rests on backfill material; the same material is used to fill the footer trench. A region of undisturbed soil is assumed to extend 10 m beyond and below the footer. The soil is assumed homogeneous and isotropic except for certain simulations in which soil layers of high permeability or radium content are introduced. Depressurization of the house induces a pressure field in the soil and backfill. The Laplace equation, resulting from Darcy's law and the continuity equation, is solved using a steady-state finite-difference model to determine this field. The mass-transport equation is then solved to obtain the diffusive and convective radon entry rates through the slab, the permeable stem wall, gaps at the intersections of the slab, stem wall, and footer, and gaps in the slab. These rates are determined for variable soil, backfill, and stem wall permeability, slab opening width and position, soil, slab, and stem wall radium content, slab and stem wall diffusivity, and water table depth. The variations in soil permeability and radium content include cases of horizontally stratified soil. We also consider the effect of a gap between the edge of the slab and the stem wall that restricts the passage of soil gas from the stem wall into the house. The model predicts that the total radon entry rate is relatively low unless the soil or backfill permeability or radium content is high. Variations in most of the factors, other than the soil permeability and radium content, have only a small effect on the total radon entry rate. However, for a fixed soil permeability, the total radon entry rate may be reduced by a factor of 2 or more by decreasing the backfill permeability, by making the stem wall impermeable and gap-free, (possibly by constructing a one-piece slab/stem-wall/footer), or by increasing the pressure in the interior of the stem wall (by ensuring that there is a large pressure drop across the slab/stem-wall gap), thereby reducing radon entry into the wall from the soil. Use of an impermeable stem wall and a low-permeability fill in combination is predicted to reduce the radon entry rate by 71%.

Nomenclature

Symbol	Name	Units
C	Radon concentration	Bq m ⁻³
C _∞	Radon concentration far from the soil surface	Bq m ⁻³
D	Radon diffusivity (bulk)	m ² s ⁻¹
E _s	Entry rate of soil gas	m ³ s ⁻¹
E _r	Normalized entry rate of radon	m ³ s ⁻¹
g	Gravitational constant	m s ⁻²
k	Air permeability	m ²
n	Number of bends in gaps or openings	-
P	Absolute pressure	Pa
P _A	Atmospheric pressure	Pa
p	Disturbance pressure	Pa
r	Radial coordinate	m
S	Radon production rate	Bq s ⁻¹
t	Thickness of gap or opening	m
w	Width of gap or opening	m
z	Vertical coordinate, positive downward	m
\vec{v}	Velocity	m s ⁻¹
ΔP	Difference between house and atmospheric pressures	Pa
ΔP _g	Pressure drop through a gap	Pa
ε	Porosity	-
λ	Radon decay rate	s ⁻¹
μ	Viscosity of air	kg m ⁻¹ s ⁻¹
ρ	Density of air	kg m ⁻³
σ	Element of area of gap or opening	m ²

Introduction

Indoor radon (²²²Rn) concentrations arise from convective flow of radon-bearing gas from soil into the building interior, diffusion of radon from soil and building materials, and from the entry of outside air (Nazaroff *et al.* 1988; Nero and Nazaroff 1984; DSMA 1983). In houses with elevated radon concentrations, convective flow of soil gas is the dominant source in almost all cases. In this situation, flow of gas, in response to a pressure difference between the soil and the building interior, will depend on both the type and location of openings or other flow pathways between the building and soil and on the characteristics of the surrounding soil. The building substructure -- usually either a basement, slab-on-grade, or crawlspace (or some combination of these) -- has a significant role in defining the nature of these pathways and openings.

As in other regions of the U.S., elevated indoor radon concentrations have been observed in a number of areas of Florida (Geomet 1988). In response, the State of Florida, along with the U.S. Environmental Protection Agency, has established the Florida Radon Research Program with the broad objectives of conducting research on radon entry into Florida housing and of developing building codes and construction standards designed to restrict radon entry into buildings (Sanchez *et al.* 1990). Since a large fraction of houses built in the state utilize one of several variants of slab-on-grade construction (Scott and Findlay 1983; Acres 1990), much of the research and code development has focused on these substructures. An important objective is to understand how details of the construction techniques used, both those in current practice and those that might be adopted in response to new building and construction codes, affect indoor radon concentrations.

We have developed a steady-state finite difference model of radon transport through soils and into buildings (Loureiro *et al.* 1990; Revzan *et al.* 1991a) to investigate the dependence of radon and soil gas entry on a variety of parameters, including features of the soil and building system. For the present study, the steady-state finite difference model has been modified to account for the details of one form of the slab-on-grade substructure. We neglect the effect of variations in atmospheric pressure, which may increase radon entry rates, especially when the soil permeability is relatively low (Narasimhan *et al.* 1990; Tsong and Narasimhan 1991). For this study, we also neglect the effect of inhomogeneity and anisotropy of soil permeability. Preliminary modeling indicates that anisotropy of soil due to layering produces significantly increased radon entry rates. Inhomogeneities such as soil fractures, which have not yet been studied, are also likely to increase entry rates. Validation of the model under controlled conditions is proceeding (Fisk *et al.* 1989; Garbesi *et al.* 1992).

We present here the predictions of the steady-state model, using a set of building substructure and soil characteristics that are representative of a particular type of Florida house. We then discuss the influence of variations in certain of these characteristics on soil gas and radon entry. Because the model is not yet validated, the results should be viewed as providing a measure of the relative, rather than absolute, effect of varying these parameters.

Model Description

We model soil-gas and radon transport for a system comprising undisturbed soil, soil backfill, and building substructure. The model incorporates an above-grade concrete slab floor, supported at the perimeter by a concrete-block stem wall that rests on a concrete footing. The slab and footing are considered to be impermeable to air, but the air permeability of the stem wall may exceed that of the soil. The stem wall is represented by inner ("house-side") and outer ("soil-side") permeable layers separated by an open zone. The sections that connect the layers are neglected and the layers are assumed continuous, *i.e.*, the changes in permeability at the mortar joints between blocks are ignored.

The slab rests on fill material elevated above the natural grade level. The footer trench is filled with the same material. The region modeled includes the slab, stem wall, and footer of the house, the fill, and a section of the undisturbed soil.

Radon-bearing air ("soil gas") is assumed to enter the interior of the stem wall through gaps between the stem wall and footer, through gaps between the stem wall and slab, and through the parts of the permeable sides of the concrete blocks that are in contact with the fill material. Air also enters the above-surface part of the soil-side concrete-block layer without passing through the soil or fill. All air entering the interior of the stem wall is assumed to pass into the house through a gap between the stem wall and the slab edge. Soil gas may also enter the house directly through an opening in the slab itself, *e.g.*, a crack or an opening for utilities. A detail of the neighborhood of the stem wall, with the width of the gaps greatly exaggerated, is shown in Figure 1. For simplicity, The walls of the footer trench have been modeled as vertical, rather than sloping. The part of the house above the slab is not modeled.

Assuming that the cross-section of the stem walls is uniform, and assuming that we are willing to limit the discussion of slab openings to those that are cylindrically-symmetrical, the slab, stem walls, and footers can be modeled as cylinders with only the loss of corner effects, which have been shown to be unimportant in the case of basements (Revzan *et al.* 1991a). The region from which a house draws soil gas depends on the positions of adjacent houses, the extent of their depressurization, and the characteristics of the soil. The exact boundaries of this region are likely to be important in particular cases, but in the general case, the soil may be represented as well by a cylinder as by a box. The entire region may therefore be modeled in cylindrical coordinates, which permits greater resolution, shorter solution time (with lower cost), or a combination of the two.

We use a finite-difference steady-state model (Loureiro 1987; Loureiro *et al.* 1990; Revzan *et al.* 1991a) that, assuming isothermal soil conditions, comprises two difference equations, each of which is obtained from a differential equation. First, the pressure field is found from Darcy's law,

$$\vec{v}(r,z) = - \frac{k(r,z)}{\mu} \nabla p(r,z), \quad (1)$$

where \vec{v} is the bulk velocity (flow rate divided by total cross-sectional area), k is the permeability of the soil, μ the viscosity of air ($1.8 \times 10^{-5} \text{ kg m}^{-1} \text{ s}^{-1}$), and r and z are the radial and vertical coordinates, respectively. The disturbance pressure, p , *i.e.*, the pressure change in the soil that is produced by the difference between house and atmospheric pressures, is defined by

$$p(r,z) = P(r,z) - P_A - \rho g z, \quad (2)$$

where P is the absolute pressure, P_A the atmospheric pressure, assumed constant in a steady-state model, ρ the density of air, which is constant when conditions are

isothermal, and g the gravitational acceleration. Under isothermal conditions, the equation of continuity may be written

$$\nabla \cdot \vec{v}(r, z) = 0. \quad (3)$$

Combining Equations 1 and 3, we have the first equation of the model:

$$\nabla \cdot \left\{ \frac{k(r, z)}{\mu} \nabla p(r, z) \right\} = 0. \quad (4)$$

The boundaries for the solution of Equation 4 are shown in Figure 2. They include the outer limits of the soil block (chosen 10 m from the footer in both the r - and z -directions, far enough from the house that insignificant change in radon entry rate results from their extension), the soil surface, the bottom of the slab, the outer surfaces of the footer, the inner surfaces of the permeable concrete blocks of the stem wall, including the parts forming the sides of the gaps, the interfaces between gaps or openings and the backfill, and the outside of the part of the stem wall that is above the soil surface. Since the area modeled does not extend above the slab, the top of the soil-side stem wall layer is treated as a boundary. Transport within the slab and footer is excluded from the model, *i.e.*, the velocity is set to zero at all nodes in these regions. Special techniques, described below, are used to determine the velocities in gaps and openings, since numerical modeling of such areas offers no advantages to offset the considerable decrease in computing speed.

At the outer soil boundaries and at all concrete surfaces, the normal derivative of the pressure must vanish, *i.e.*, there is no flow of air across these boundaries. At the soil surface, the disturbance pressure vanishes. At the backfill side of each of the gaps shown in Figure 2, the pressure is determined by the difference between the house pressure and the pressure drop through the gap. Temperature differences between a house and the outside, the effect of wind, and the operation of heating, ventilation, and air-conditioning systems produce a pressure at the floor which is generally lower than P_A (Feustel and Sherman 1989; Sherman *et al.* 1979; see also Revzan *et al.* 1988; Revzan 1989). The difference between the house pressure and P_A , ΔP , is assumed to be the pressure at the top of the slab. In the general case, ΔP is also assumed to be the pressure inside the stem wall. Two special cases are also considered: 1) the stem wall is impermeable, so that the normal derivative of the pressure vanishes at the stem wall; 2) there is considered to be a restriction between the inside of the stem wall and the house (*i.e.*, the gap between the edge of the slab and the inside of the stem wall is small), so that the pressure inside the stem wall is the difference between ΔP and the pressure drop caused by flow through the restriction.

The pressure drop through a gap, ΔP_g , is determined from an algorithm due to Baker (Baker *et al.* 1989):

$$|\Delta P_g| = \frac{12\mu t}{w^2} |v| + \frac{\rho(1.5+n)}{2} v^2. \quad (5)$$

Here, t is the length of the gap in the direction of flow, w is the width of the gap perpendicular to the flow, v is the average speed of air in the gap, *i.e.*, the flow rate through the gap divided by the area, and n is the number of bends in the gap (always 0 for the configuration discussed here). For a restriction between the house and the interior of the stem wall, treated as a gap, the flow into the gap is determined by summing all flows into the interior of the wall through the permeable inner and outer layers and the wall-footer and wall-slab gaps. This summed flow also includes the flow of outside air, considered to be radon-free, through the above-grade part of the wall. Air flow through the permeable layers is not, in general, horizontal, *i.e.*, parallel to the soil surface, so that air can flow from a layer into a gap. Such a flow cannot be incorporated into Equation 5, so that we have excluded it from the model by requiring that the edges of gaps in the stem wall layers be no-flow boundaries, as shown in Figure 2. This choice of boundary condition is unlikely to affect total radon entry rates significantly, but it does slightly exaggerate the fraction of radon entering through the layers at the expense of the fraction entering through the gaps. The top of the soil-side stem wall layer is also treated as a no-flow boundary.

Once a solution to Equation 4 is obtained, the soil-gas velocity is found from Equation 1 and the soil-gas entry rate, E_s , from

$$E_s = \int_{\Sigma} \vec{v}(r_g, z) \cdot d\vec{\sigma}(r_g, z), \quad (6)$$

where $\vec{\sigma}$ is an element of area and Σ indicates an integral over the entire area of interest. In the case of the soil-side stem wall layer, the soil-gas entry rate is found by subtracting the air flow through the above-grade part of the outside surface of the layer from the total air and soil-gas flow through the inside surface. In practice, we calculate soil-gas entry rates through each of the gaps, through the house-side stem wall layer, and through the soil-side stem wall layer. In addition, we calculate the flow rate of air through the soil surface for comparison with the total soil-gas entry rate through all gaps and permeable walls.

After the pressure field in the soil, permeable stem wall layers, and gaps or openings is found from Equation 4, the radon concentration, C , may be obtained from the steady-state mass-transport equation (Nazaroff *et al.* 1988),

$$\vec{v}(r, z) \cdot \nabla C(r, z) = \nabla \cdot [D(r, z) \nabla C(r, z)] - \epsilon(r, z) \lambda C(r, z) + \epsilon(r, z) S(r, z), \quad (7)$$

where ϵ is the porosity, D the bulk radon diffusivity (the effective diffusivity is found by dividing D by ϵ), λ the radon decay constant, and S the rate of release of radon per unit pore space volume. For gaps and openings, we assume $\epsilon = 1$ and $S = 0$. For any material, the theoretical maximum concentration at distances far from the influence of

surface boundary conditions, C_{∞} , is given by

$$C_{\infty} = \frac{S}{\lambda}. \quad (8)$$

In general, the radon concentration in materials other than the undisturbed soil is less than C_{∞} for that material.

The boundaries for the solution of Equation 7 are shown in Figure 3. They include the outer soil boundaries, the soil surface, the basement side of the slab, the interior of the stem wall, and the portion of the stem wall exterior that is above the soil surface. At the soil surface, we assume $C = 0$; because radon concentrations in soil gas are typically high compared to those in the atmosphere, the assumption of a non-zero soil-surface concentration has a negligible effect on the result. We also assume $C = 0$ inside the stem wall, since the flow of low-radon air through the soil-side layer is much greater than the flow of high-radon air through the house-side layer. At the outer and lower boundaries of the soil, we assume that the normal derivative of C vanishes, which is equivalent to the assumption that there is no passage of radon by diffusion across these boundaries. Since passage of radon by convection has been excluded by the boundary conditions used in solving Equation 4, these are no-flow boundaries for radon. In the special case of an impermeable stem wall, the boundary is the top of the wall, which is an extension of the slab. The interior of the stem wall, whose radon concentration is no longer zero, is included in the region of the model.

From previously-determined velocities and a solution to Equation 7, we find the radon entry rate, E_r , and the average radon concentration, $\langle C \rangle$, for any entry area of interest, from the equations

$$E_r = \int_{\Sigma} [\vec{v}(r,z)C(r,z) - D \nabla C] \cdot d\vec{\sigma}(r,z) \quad (9)$$

and

$$\langle C \rangle = \frac{\int_{\Sigma} C(r,z) d\sigma(r,z)}{\int_{\Sigma} d\sigma(r,z)}, \quad (10)$$

where σ and Σ have the same meaning as for Equation 6.

Procedures

We define a "base configuration" for the substructure, soil, and fill. The characteristics of the base substructure were determined from a review of typical construction practices (Acres 1990; Scott and Findlay 1983) and in discussions with Florida researchers; the base-case soil and fill properties were determined from available studies of soil and fill properties (Nielsen and Rogers 1990; Roessler *et al.* 1990). In this configuration (Figure 1), the outer edge of the concrete-block wall is 7 m from the center of the slab and the concrete blocks are 0.19 m wide in total, with a central air space of 0.134 m and two concrete layers 0.028 m thick. The slab is 0.1 m thick. The footer is 0.45 m wide by 0.30 m high. There are gaps between the inside layer of the stem wall and the slab, between the inside layer of the stem wall and the footer, and between the outside layer of the stem wall and the footer; each of these gaps is 0.003 m wide. There is an opening in the slab 3 m from the center; this opening, representing a crack or joint, is also 0.003 m wide.

The distance between the bottom of the slab and the soil surface is 0.3 m and that between the soil surface and the top of the footer is 0.2 m. The regions between the bottom of the slab and the soil surface and between the top of the footer and the soil surface (the footer trench) are assumed to contain a backfill material that may be different from the undisturbed soil. The outer edge of the soil is 10 m beyond the outer edge of the footer, i.e., 17.13 m from the center of the slab. The depth of the soil block is 10 m greater than the bottom of the footer, i.e., 10.5 m below the soil surface or 10.9 m below the top of the slab. These distances are great enough that no significant increase in the radon entry rate results from their extension.

The base-case permeabilities, diffusivities, pore-space radon concentrations, and porosities of the materials included in the model are shown in Table 1. The indicated radon concentration is C_{∞} , as defined by Equation 8, for the material of interest. The proximity of the slab and stem wall layers to low-concentration regions ensures that concentrations in these concrete materials are lower than C_{∞} ; the concentration in the soil approaches C_{∞} at a depth of a few meters below the surface.

The pressure at the top of the slab is fixed at -2.4 Pa with respect to the atmosphere, which is a typical indoor-outdoor pressure difference. This is also the pressure in the interior of the stem wall, except for the special cases of an impermeable stem wall and a flow-restrictive gap between the slab edge and the stem wall.

A list of simulations is given in Table 2. In each case the parameter indicated in column 1 is varied over the range given in column 2, the other parameters retaining their base values except where noted. The number of simulations carried out for each parameter is shown in column 3. For 19 of the entries in Table 2, all parameters retain their base values except for the one indicated as varying; in 2 cases, all stem-wall gaps are closed; in 2 cases, an impermeable stem wall is simulated, as described in the previous section; in 2 cases, the permeability of the backfill material is different from the base value; in 1 case, entry through the two gaps between the stem wall and the footer (Figure 1) is

excluded.

Results and Discussion

The Base Configuration

For the base configuration, the predicted air and soil-gas entry rate into the house through the substructure is $6.9 \times 10^{-3} \text{ m}^3 \text{ s}^{-1}$, of which 93% is outside air that enters the soil-side of the stem wall. The soil-gas entry rate is $4.5 \times 10^{-4} \text{ m}^3 \text{ s}^{-1}$. As a check on the mass-balance, the flow of air across the soil surface is calculated. This differs from the total soil-gas entry rate by less than 0.005%, which indicates that the mass-balance is within acceptable limits. The percentage of the soil gas that enters through each of the areas of interest is shown in Table 3. 92% of the total entry is through the soil side of the stem wall, including the gap, 6% through the house side of the stem wall, including the gaps, and 2% through the slab opening. The flow of outside air through the above-surface part of the stem wall is a factor of 14 greater than the total flow of soil gas through the remainder of the entry areas.

The predicted radon entry rate into the house is 2.3 Bq s^{-1} . If there is no pressure difference between the inside and outside of the house, the predicted entry rate is 1.2 Bq s^{-1} , so that 1.1 Bq s^{-1} may be attributed to convection. This "convective" entry rate may not be due entirely to convection in the strict sense, but may also include an increase in the diffusive entry rate caused by an increased radon concentration at the point of entry, this in turn being caused by the additional flow of radon-bearing soil gas into the vicinity of the substructure. The percentages of the diffusive, convective (in the sense of the previous sentence), and total radon entry rates through each of the areas of interest are shown in Table 3. The average radon concentration for each of the areas as a fraction of C_∞ is also shown; this is to be understood as the concentration at the soil side of each of the areas, since the concentrations at the house side of the slab and the interior of the stem wall are assumed to be zero.

Of the diffusive entry, 43% is through the house side of the stem wall, including the two gaps, 4% is through the soil side of the stem wall, including the gap, 10% is through the slab opening, and 43% is through the slab. Of the non-diffusive entry, 56% is through the house side of the stem wall, including the two gaps, 24% is through the soil side of the stem wall, including the gap, 17% is through the slab opening, and 2% is through the slab. The "convective" entry through the slab is not truly convective, since that is excluded by our choice of boundary conditions, but is rather an increase in diffusive entry. Of the total radon entry, 50% is through the house side of the stem wall, including the two gaps, 14% is through the soil side of the stem wall, including the gap, 13% is through the slab opening, and 23% is through the slab. The differences between the fractional soil-gas and radon entry rates at the several entry points are due to the differing radon concentrations in the soil gas at the several points of entry; these differences are due, in turn, primarily to the differing flow-path lengths from soil surface to

opening. The radon concentration at the soil side of the stem wall is $0.02 C_{\infty}$ or less, depending on proximity to the surface. At the inner wall, the concentration is $0.64 C_{\infty}$, while at the slab the concentration rises to $0.77 C_{\infty}$.

The soil-gas and radon entry rates that are predicted by the model when certain parameters are varied from their base values are shown in Table 2. In each case, the parameter under consideration is shown in column 1; any other conditions that are different from the base configuration are shown in parentheses. In every case, the discrepancy between the total soil-gas entry rate and the entry rate of air at the soil surface is less than 0.01%.

Of those parameters that are under the control of builders, only the permeability and radium concentration of the fill, the stem wall characteristics, the width of the slab/stem-wall gap, and the radium concentration and effective radon diffusivity of the slab have a significant influence on the radon entry rate. Since the characteristics of concrete are well understood and, in any case, diffusive entry from concrete is rarely the principal source of radon in high-radon houses, the final two parameters will not be discussed further. We describe the influence of the other important controllable parameters on radon entry in the following sections; for a full discussion of all of the results summarized in Table 2, see (Revzan *et al.* 1991b). A summary of the significant results is provided in Table 4.

Fill Characteristics

If the permeability of the fill is reduced from its base value of $4 \times 10^{-11} \text{ m}^2$ to 10^{-13} m^2 , the total radon entry rate diminishes from 2.33 to 1.23 Bq s^{-1} , a 47% reduction. The diminution in the entry rate resulting from further reduction of the fill permeability is insignificant. Diffusive radon entry through the slab is affected by changes in the fill permeability only to the extent that the radon concentration on the fill side of the slab is changed. If this mode of entry is excluded, the radon entry rate changes from 1.79 to 0.72 Bq s^{-1} when the fill permeability is decreased, a 60% reduction. Since the slab is unlikely to be the principal source of radon in high-radon houses, this 60% reduction is more indicative of the importance of the fill permeability than is the 47% reduction in the total radon entry rate. The low-permeability fill exerts a controlling influence on soil-gas flow, so that the radon entry rate is now essentially unaffected by the soil permeability. At the very high soil permeability of 10^{-9} m^2 , the introduction of the low-permeability fill reduces the total radon entry by 91% from the base value. Increasing the fill permeability to 10^{-9} m^2 increases the total radon entry rate by 14% over the base case and the radon entry rate exclusive of diffusive entry through the slab by 15%. The change in entry rate resulting from further increase in the fill permeability is insignificant. The total radon entry rate and the entry rates through the house and soil sides of the stem wall and the slab opening are plotted against the fill permeability in Figure 4. (The entry rate by diffusion through the slab has been excluded to improve the clarity of the figure; the range of diffusive entry rates through the slab is 0.51 to 0.55 Bq s^{-1} .)

If the radium content of the fill material is reduced by an order of magnitude, both the total radon entry rate and the radon entry rate exclusive of diffusive entry through the slab are reduced by 19%. The smallness of the reduction in radon entry produced by the large, and probably impractical, reduction in radium, is the consequence of the diffusion and convection of high-radon soil gas into the fill from the undisturbed soil. If the fill material is also of low permeability (10^{-13} m^2), the reduction in the total radon entry rate from the base value is 58% and the reduction in the entry rate exclusive of diffusion through the slab is 69%.

If the radium content of the fill is increased by a factor of 5 over the base case, the total radon entry rate is increased by 83% (the radon entry rate exclusive of diffusion through the slab is increased by 85%). When the increase is by a factor of 10, the entry rate increase becomes 188% (124%). A further indication of the importance of a high-radium fill is provided by a configuration whose soil has a permeability two orders of magnitude below the base value (*i.e.*, 10^{-13} m^2) but whose fill has a radium content 5 times the base. The predicted total radon entry rate is 2.64 Bq s^{-1} , which is 13% higher than the base value and 90% higher than the value for a configuration with low-permeability soil and normal (base value) fill radium. Of this entry rate, 88% is diffusive, so that the high-radium fill produces a radon entry rate essentially equal to the base value no matter how low the soil or fill permeability may be. Finally, if both the fill and soil have radium contents a factor of 5 greater than the base value, with their permeabilities retaining their base values, the predicted total radon entry rate is 187% greater than the base value and 57% greater than the value when only the fill has a high radium content.

Based on the predictions of the model, the use of low-permeability backfill material will reduce radon entry significantly. The use of low-radium material is not necessary, but it is important to avoid material that is much higher in radium than the undisturbed soil.

Stem-wall Characteristics

Elimination of all convective radon entry in the vicinity of the stem wall, as might be accomplished by making the slab, stem wall, and footer a single concrete unit (sometimes referred to as a "monolithic slab"), reduces total radon entry by 53% and radon entry exclusive of diffusive entry through the slab by 68%. The radon entry rate for this configuration is not identical to the sum of the entry rates through the slab and slab opening in the base configuration. The effective elimination of the stem wall as an influence on the pressure field in the soil increases the pressure gradient near the slab, particularly near the opening, so that the entry rates through the slab and slab opening increase, the former from 0.54 to 0.57 Bq s^{-1} and the latter from 0.30 to 0.52 Bq s^{-1} . If the low-permeability (10^{-13} m^2) fill is combined with the impermeable stem wall, the total radon entry rate is reduced by 71% and the entry rate exclusive of diffusion through the slab by 94%.

It is probably unrealistic to expect that the impermeable stem wall would remain unaffected by normal cracking. To simulate the effect of cracks, we have introduced into the model a second opening in the concrete slab, this one placed at the junction of the slab and stem wall. The width of the opening is identical to the width of the central opening in the slab, *i.e.*, 0.003 m. (Opening width has only a small effect on radon entry; see Table 2.) With this opening present, making the stem wall impermeable reduces the total radon entry rate by 33% from its base value, instead of the 53% obtained when the second opening is absent; the reduction in the entry rate exclusive of diffusion through the slab is 44%, instead of 68%. When the fill is of very low permeability (10^{-15} m², the total entry rate is reduced by 64% from the base rate (71% without the second opening) and the entry rate exclusive of diffusion through the slab by 84% (94%).

Restriction of Soil-gas Flow from Stem-Wall Interior to House

When the interior of the stem wall is at less than atmospheric pressure, there is a considerable flow of outside air through the part of the outer (soil-side) layer that is above the soil surface, in addition to the flow through the below-grade part (Figure 1). For the base configuration, the flow rate of outside air is 6.2×10^{-3} m³ s⁻¹, which is a factor of 14 greater than the total flow of soil gas into the house. If there is a small gap between the edge of the slab and the outer layer, *i.e.*, a flow restriction between the stem wall interior and the house, the pressure drop through the gap will cause the pressure in the stem wall interior to be greater (*i.e.*, less negative with respect to atmospheric pressure) than that in the house, so that the driving force of soil gas and radon entry through the stem wall, wall-footer gaps, and wall-slab gap will be diminished. (If air is permitted to flow vertically through the soil side of the stem wall, the flow restriction may be partially bypassed. In the model, we have used a no-flow boundary condition at the top of the soil side of the stem wall; in practice, sealing of this area may be necessary to prevent vertical flow.)

For gap widths less than 0.0008 m, the pressure on the house side of the stem wall is less than that in the interior, so that air and soil gas may flow through the concrete blocks from the soil side to the house side (below the slab) without entering the house, so that radon entry rates through the stem wall are uncertain, but likely to be near zero. At a gap width of 0.0005 m, the total radon entry rate is reduced by 50% or more from the base value, and the entry rate through the stem wall by 95% or more, so that almost all of the radon entry is through the slab or the slab opening. The increased flow of soil gas beneath the slab causes the entry rate through the slab opening to increase by 83% over the base value, so that flow restriction is less effective in reducing radon entry than is the elimination of soil-gas flow through the stem-wall, *e.g.*, by using a monolithic slab. The pressure drop through the gap is 2.2 Pa or 92% of the house depressurization. At a gap width of 0.001 m, the pressure drop is 58% of the house pressure, the radon entry rate through the stem wall is reduced by 46% and the total radon entry rate by 21% from the base values.

It is possible to bring the interior stem wall pressure even closer to atmospheric pressure by increasing the permeability of the above-surface part of the soil side of the stem wall. If the remaining parts of the wall are maintained at low permeability, the radon entry rate through the wall may be greatly diminished. For the base configuration, with a slab-stem wall gap of 0.001 m, an above-surface wall permeability of 10^{-9} m^2 , and the remainder of the wall of permeability 10^{-12} m^2 , the pressure drop through the gap is 2.2 Pa (92% of base), the total radon entry rate is 1.14 Bq s^{-1} , a reduction of 51%, and the entry rate through the stem wall is just 0.07 Bq s^{-1} a reduction of 96%. These values are similar to those obtained for the 0.0005 m gap with the stem wall retaining its base permeability.

Conclusions

For the base configuration, the predicted radon entry rate is 2.3 Bq s^{-1} , equivalent to a flux of 0.015 Bq s^{-1} per m^2 of slab area. For one-story houses with air exchange rates from $0.5\text{-}1.0 \text{ h}^{-1}$, this flux produces indoor concentrations of $20\text{-}40 \text{ Bq m}^{-3}$. These values are consistent with concentrations observed in Florida houses (Geomet 1988).

Of the total radon entry rate in the base configuration, 52% is attributable to diffusion, *i.e.*, the radon entry rate would be 1.2 Bq s^{-1} when the house is at atmospheric pressure. When the house pressure is 2.4 Pa below atmospheric, the radon entry increases to 2.3 Bq s^{-1} . The increase is due to convective entry of radon-bearing soil gas and to an increase in diffusive entry due to a higher radon concentration in the pore spaces of the material adjacent to the slab and stem wall. 64% of the total radon entry and 80% of the radon entry attributable to house depressurization occurs through the stem wall blocks or gaps between the stem wall blocks and the slab or footer. Although these numbers are slightly misleading, because elimination of an entry point does not result in the reduction of radon entry by the amount entering through that point, they do suggest that attention be paid to the area of the stem wall. The use of a monolithic slab reduces total radon entry by 53%.

Examination of the effect on radon entry of changes in the house substructure and materials in the the adjacent region indicates that attention should also be paid to the permeability of the backfill. The use of a backfill of permeability 10^{-13} m^2 or less not only reduces total radon entry by 47%, but almost eliminates the dependence of radon entry on soil permeability. Combining the low-permeability fill with the monolithic slab reduces total radon entry by 71%.

The radium content of the backfill is important only if it is significantly higher than that of the near-surface soil. An increase by a factor of 5 over the base value (and over the soil radium content) produces a 83% increase in total radon entry, whereas a reduction by a factor of 5 reduces radon entry by just 19%. If the radium content of both fill and soil is increased by a factor of 5, radon entry increases by nearly a factor of 4. However, increasing the radium content of the soil alone has a smaller effect on radon entry.

In particular, the radium content of the soil 5 m or more below the surface has little influence on radon entry.

Acknowledgments

This work was supported by the U.S. Environmental Protection Agency (EPA) through Interagency Agreement DW89934620-0 with the U.S. Department of Energy (DOE). This work was also supported by the Assistant Secretary for Conservation and Renewable Energy, Office of Building Technologies, Building Systems and Materials Division and by the Director, Office of Energy Research, Office of Health and Environmental Research of DOE under contract DE-AC03-76SF00098. Although the research described here is partially supported by the EPA, it has not been subjected to EPA review and therefore does not necessarily reflect the views of EPA, and no official endorsement by EPA should be inferred.

References

- Acres International Corporation. Radon Entry Through Cracks in Slabs-on-Grade, Vol. 2, Sealants for Cracks and Openings in Concrete Slabs-On-Grade. Amherst, NY: Acres Report P09314; 1990.
- Baker, P.H.; Sharples, S.; Ward, I.C. Air Flow Through Cracks. *Building and Environment*, 22(4), 293-304; 1989.
- DSMA Atcon Ltd. Review of Existing Instrumentation and Evaluation of Possibilities for Research and Development of Instrumentation to Determine Future Levels of Radon at a Proposed Building Site. Ottawa, Canada: Atomic Energy Control Board Report INFO-0096; 1983.
- Feustel, H.E.; Sherman, M.H. A Simplified Model for Predicting Air Flow in Multizone Structures. *Energy and Buildings*, 13, 217-230; 1989.
- Fisk, W.J.; Flexser, S.; Gadgil, A.J.; Holman, H.-Y.; Modera, M.P.; Narasimhan, T.N.; Nuzum, T.; Revzan, K.L.; Sextro, R.G.; Smith, A.R.; Tsang, Y.W.; and Wollenberg, H.A. Monitoring and Modeling for Radon Entry into Basements: A Status Report for the Small Structures Project. Berkeley, CA: Lawrence Berkeley Laboratory Report LBL-27962; 1989.
- Garbesi, K.; Sextro, R.G.; Fisk, W.J.; Modera, M.P.; Revzan, K.L. Soil-gas Entry into an Experimental Basement: Model-measurement Comparisons and Seasonal Effects. Berkeley, CA: Lawrence Berkeley Laboratory Report LBL-31873; 1992. To be published in *Environmental Science and Technology*.
- Geomet Technologies Inc. Florida Statewide Radiation Survey. Germantown, MD: Geomet Report IE-1808; 1988.
- Loureiro, C.deO. Simulation of the Steady-State Transport of Radon from Soil into Houses with Basements under Constant Negative Pressure. Berkeley, CA: Lawrence Berkeley Laboratory Report LBL-24378; 1987.
- Loureiro, C.deO.; Abriola, L.M.; Martin, J.E.; and Sextro, R.G. Three Dimensional Simulation of Radon Transport into Houses Under Constant Negative Pressure. *Environ. Sci. Technol.* 24, 1338-1348; 1990.
- Narasimhan, T.N.; Tsang, Y.W.; Holman, H.Y. On the Potential Importance of Transient Air Flow in Advective Radon Entry Into Buildings. *Geophys. Res. Letters* 17, 821-824; 1990.
- Nazaroff, W.W.; Moed, B.A.; Sextro, R.G. Soil as a Source of Indoor Radon: Generation, Migration, and Entry. In Nazaroff, W.W. and Nero, A.V., eds., *Radon and Its Decay Products Indoors*; New York: Wiley; 1988; 57-112.
- Nero, A.V.; Nazaroff, W.W. Characterizing the Source of Radon Indoors. *Radiation Protection Dosimetry* 7, 23-29; 1984.
- Nielson, K.K.; Rogers, V.C. Correlation of Florida Soil-Gas Permeabilities with Grain Size, Moisture, and Porosity. Salt Lake City, UT: Rogers and Associates Report RAE-

8945-1; 1990.

Revzan, K.L.; Turk, B.H.; Harrison, J.; Nero, A.V.; Sextro, R.G. Parametric Modelling of Temporal Variations in Radon Concentrations in Homes. *IEEE Trans Nucl Sci* 35(1), 550-555; 1988.

Revzan, K.L. Radon Entry, Distribution, and Removal in Two New Jersey Houses with Basements. Berkeley, CA: Lawrence Berkeley Laboratory Report LBL-26830; 1989.

Revzan, K.L.; Fisk, W.J.; Gadgil, A.J. Modeling Radon Entry into Houses with Basements: Model Description and Validation. *Indoor Air*, 2, 173-189; 1991a.

Revzan, K.L.; Fisk, W.J.; Sextro, R.G. Modeling Radon Entry into Florida Houses with Concrete Slabs and Concrete-Block Stem Walls. Berkeley, CA: Lawrence Berkeley Laboratory Report LBL-30005; 1991b.

Roessler, C.E.; Smith, D.L.; Bolch, W.E.; Hintenlang, D.E.; Furman, R.A. Gas Permeabilities and Radon Content of Florida Fill Materials and Soils. Gainesville, FL: University of Florida Report; 1990.

Sanchez, D.C.; Dixon, R.; Williamson, A.D. The Florida Radon Research Program: Systematic Development of a Basis for Statewide Standards. Presented at the 1990 International Symposium on Radon and Radon Reduction Technology, Atlanta, GA., Paper A-I-3; to be published in the proceedings; 1990.

Scott, A.G.; Findlay, W.O. Demonstration of Remedial Techniques Against Radon in Houses on Florida Phosphate Lands. Montgomery, AL: U.S. EPA Report EPA 520/5-83-009; 1983.

Sherman, M.H.; Grimsrud, D.T.; Diamond, R.C. Infiltration-Pressurization Correlation: Surface Pressures and Terrain Effects. Berkeley, CA: Lawrence Berkeley Laboratory Report LBL-8785; 1979.

Tsong, Y.; Narasimhan, T.N. Effects of Periodic Atmospheric Pressure Variation on Radon Entry into Buildings. Berkeley, CA: Lawrence Berkeley Laboratory Report LBL-31164; 1991. Submitted to *J. Geophys. Res.*

Material	Permeability (m ²)	Bulk Diffusivity (m ² s ⁻¹)	C _∞ (Bq m ⁻³)	Porosity
Gaps and openings		1.2x10 ⁻⁵		
Concrete slab and footer		10 ⁻⁸	3.7x10 ⁴	0.2
Concrete blocks of stem wall	10 ⁻¹⁰	10 ⁻⁸	3.7x10 ⁴	0.2
Backfill	4x10 ⁻¹¹	10 ⁻⁶	3.7x10 ⁴	0.5
Undisturbed soil	10 ⁻¹¹	10 ⁻⁶	3.7x10 ⁴	0.5

1. Values of certain parameters in the base configuration.

Parameter	Range of Parameter	Number of Simulations	Soil-Gas Entry Rates ($\text{m}^3 \text{s}^{-1}$)	Radon Entry Rates (Bq s^{-1})
(Base)	-	1	4.5×10^{-4}	2.33
Soil permeability	$10^{-12} - 10^{-9} \text{ m}^2$	10	$4.0 \times 10^{-4} - 1.0 \times 10^{-3}$	1.48 - 13.4
Soil permeability (fill permeability 10^{-9} m^2)	$10^{-12} - 10^{-9} \text{ m}^2$	10	$3.3 \times 10^{-3} - 6.1 \times 10^{-3}$	1.59 - 44.4
Soil permeability (fill permeability 10^{-13} m^2)	$10^{-12} - 10^{-9} \text{ m}^2$	10	$5.0 \times 10^{-8} - 5.0 \times 10^{-8}$	1.23 - 1.23
Soil permeability (no stem-wall gaps)	$10^{-12} - 10^{-9} \text{ m}^2$	10	$3.9 \times 10^{-6} - 3.3 \times 10^{-5}$	0.97 - 1.90
Soil permeability (impermeable stem wall)	$10^{-12} - 10^{-9} \text{ m}^2$	10	$3.8 \times 10^{-6} - 3.3 \times 10^{-5}$	0.75 - 1.69
Soil permeability of 0.4-1.4 m layer	$10^{-12} - 10^{-9} \text{ m}^2$	10	$4.0 \times 10^{-4} - 9.5 \times 10^{-4}$	1.61 - 7.59
Soil permeability of 0.9-1.9 m layer	$10^{-12} - 10^{-9} \text{ m}^2$	10	$4.3 \times 10^{-4} - 5.1 \times 10^{-4}$	1.72 - 3.90
Fill permeability	$10^{-15} - 10^{-9} \text{ m}^2$	19	$5.0 \times 10^{-8} - 3.3 \times 10^{-3}$	1.20 - 2.66
Fill permeability (impermeable stem wall)	$10^{-15} - 10^{-9} \text{ m}^2$	19	$8.3 \times 10^{-10} - 4.5 \times 10^{-5}$	0.67 - 2.07
Fill permeability (no stem-wall gaps)	$10^{-15} - 10^{-9} \text{ m}^2$	19	$8.3 \times 10^{-10} - 4.5 \times 10^{-5}$	0.89 - 2.28
Soil side fill permeability	$10^{-15} - 10^{-9} \text{ m}^2$	19	$3.9 \times 10^{-5} - 3.3 \times 10^{-3}$	2.11 - 2.33
Stem wall permeability	$10^{-15} - 10^{-9} \text{ m}^2$	19	$8.3 \times 10^{-5} - 5.2 \times 10^{-4}$	1.93 - 2.35
House-side stem wall permeability	$10^{-15} - 10^{-9} \text{ m}^2$	19	$4.5 \times 10^{-4} - 4.5 \times 10^{-4}$	2.11 - 2.34
Soil-side stem wall permeability	$10^{-15} - 10^{-9} \text{ m}^2$	19	$8.9 \times 10^{-5} - 5.2 \times 10^{-4}$	2.17 - 2.34
Stem wall permeability (no wall-footer gaps)	$10^{-15} - 10^{-9} \text{ m}^2$	19	$2.9 \times 10^{-5} - 5.2 \times 10^{-4}$	1.65 - 2.25
Slab opening width	$0 - 10^{-1} \text{ m}$	8	$4.5 \times 10^{-4} - 4.5 \times 10^{-4}$	2.15 - 2.67
Slab opening distance from center	$0 - 7 \text{ m}$	8	$4.5 \times 10^{-4} - 4.5 \times 10^{-4}$	2.21 - 2.27
Water table depth	$0.5 - 10 \text{ m}$	11	$4.3 \times 10^{-4} - 4.5 \times 10^{-4}$	1.63 - 2.33
Radium concentration of fill*	$0.1 - 10$	7	4.5×10^{-4}	1.89 - 6.70
Radium concentration of soil below 1 m*	$0.1 - 10$	7	4.5×10^{-4}	1.73 - 8.36
Radium content of soil below 5 m*	$0.1 - 10$	7	4.5×10^{-4}	2.30 - 2.45
House to stem wall interior gap width	$0.0005 - 0.004 \text{ m}$	9	$4.6 \times 10^{-5} - 4.4 \times 10^{-4}$	1.17 - 2.31
Effective radon diffusivity (slab)	$10^{-9} - 10^{-6} \text{ m}^2 \text{ s}^{-1}$	10	4.5×10^{-4}	1.89 - 5.15
Radium concentration of slab*	$0.1 - 10$	7	4.5×10^{-4}	2.18 - 3.89
Effective radon diffusivity (stem wall)	$10^{-9} - 10^{-6} \text{ m}^2 \text{ s}^{-1}$	10	4.5×10^{-4}	2.31 - 2.66
Radium concentration of stem wall*	$0.1 - 10$	7	4.5×10^{-4}	2.32 - 2.49

*Relative to the remainder of the soil and/or fill

- Summary of all simulations and results. The parameters, the range of values of each parameter, the number of simulations carried out, and the ranges of total soil-gas and radon entry rates that result from variation of each parameter. Parameters other than the one varied and those indicated in column 1 retain the values of the base configuration, as described in the text and listed in Table 1.

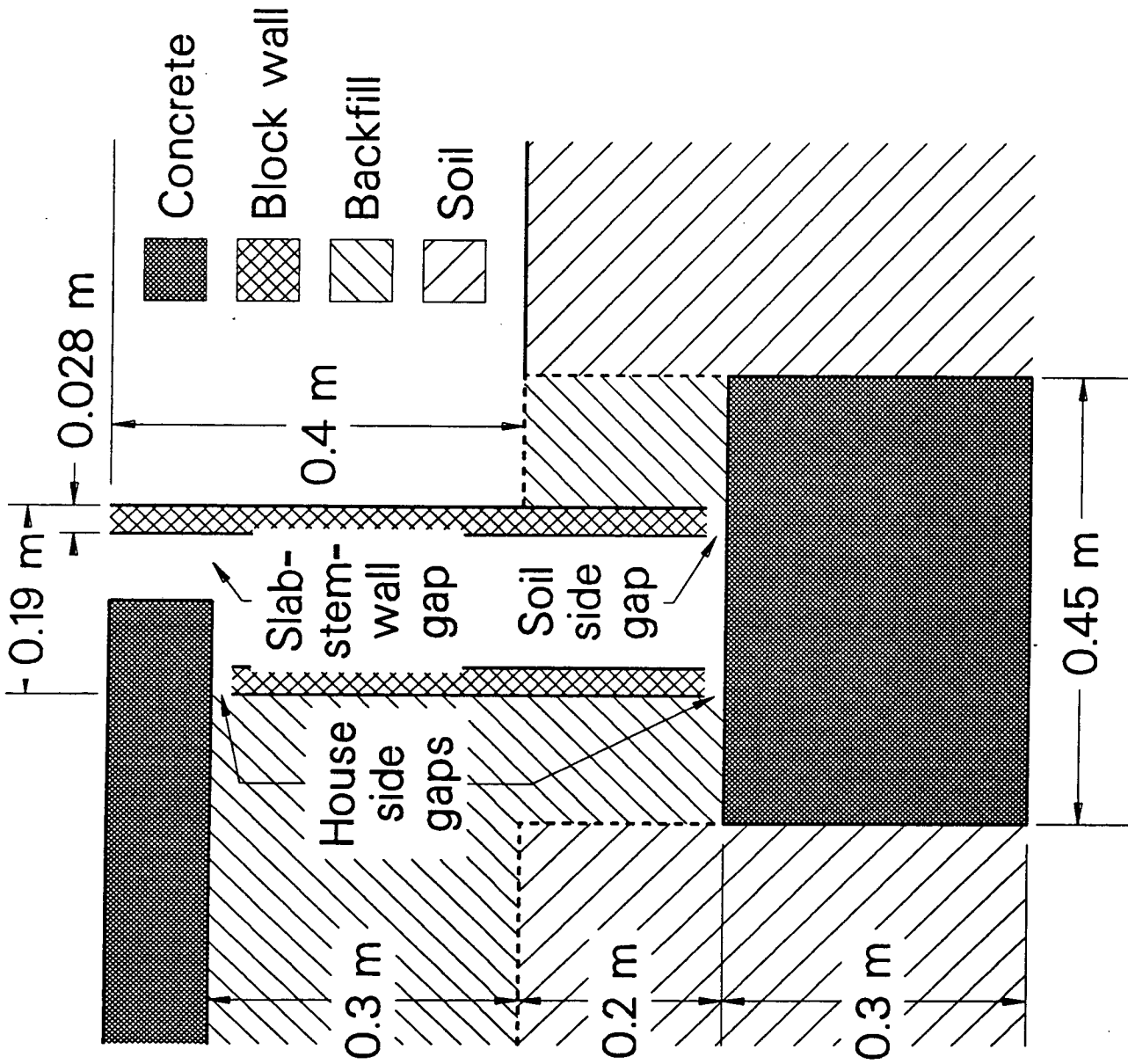
Entry Point	% of soil gas entry	Avg. radon concentration (% of C_{∞})	% of diffusive radon entry	% of convective radon entry	% of total radon entry
House side of stem wall, top gap	*	11	15	5	10
House side of stem wall, side of block	6	64	12	46	29
House side of stem wall, bottom gap	*	12	16	5	11
Soil side of stem wall, side of block	90	1	1	23	12
Soil side of stem wall, bottom gap	2	2	3	1	2
Footer			1	*	1
Slab opening	2	70	9	17	13
Slab		77	43	2	23

*less than 0.5%

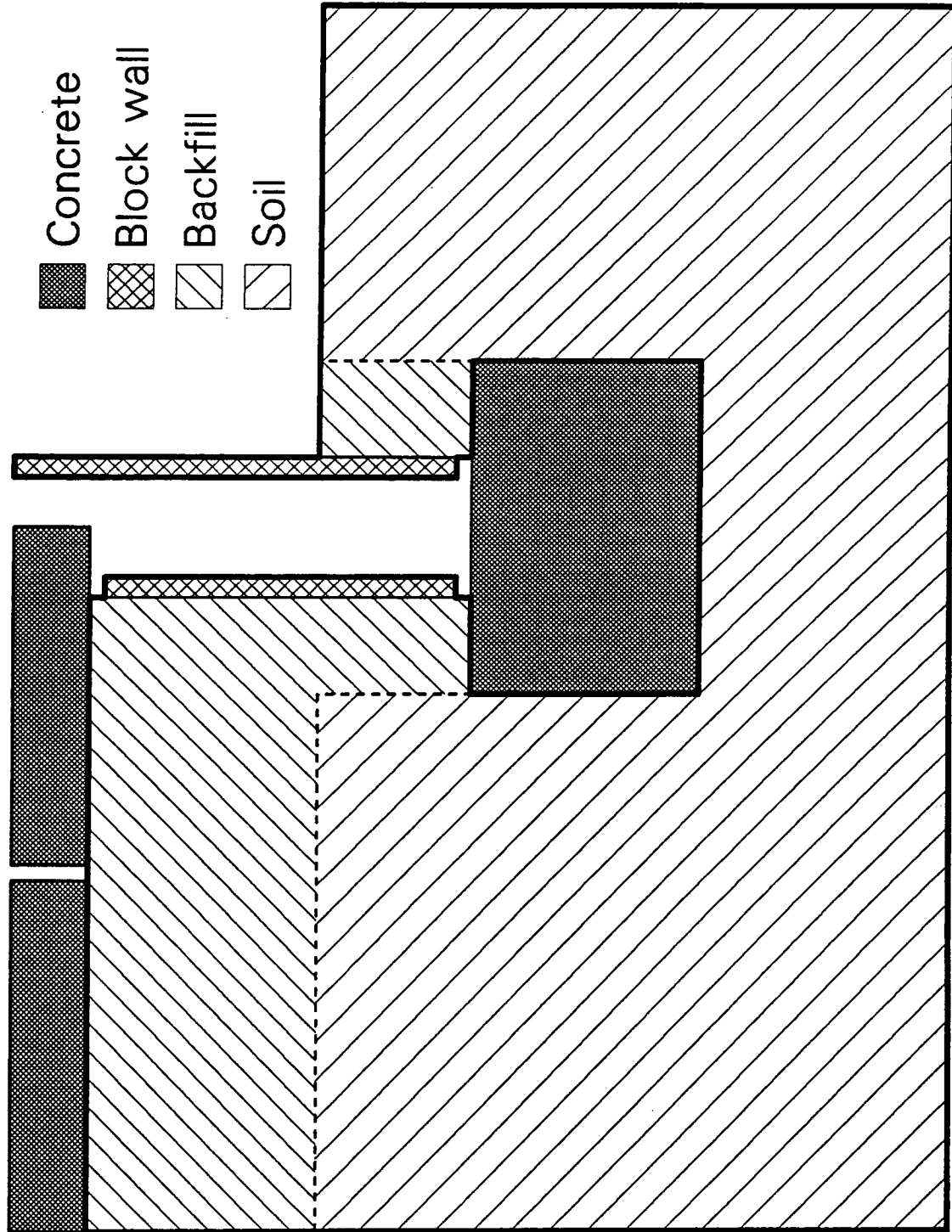
- For the base configuration, as described in the text, the percentages of the soil-gas entry rate and the diffusive, convective, and total radon entry rates for each of the entry points described in the text. The convective entry rate is defined to be the difference between the total entry rates with and without a pressure field. The radon concentration given is the average at the soil side of the entry area, as a percentage of C_{∞} ; the concentrations at the interior of the stem wall and the basement side of the slab are zero.

Configuration	Total radon entry (Bq s ⁻¹)	Radon entry, exclusive of slab (Bq s ⁻¹)
Base	2.33	1.79
Low permeability fill	1.23	0.72
Low radium fill	1.89	1.45
Low permeability fill, low radium fill	0.97	0.55
Impermeable stem wall	1.09	0.57
Impermeable stem wall, low permeability fill	0.67	0.11
Impermeable stem wall, low permeability fill, low radium fill	0.54	0.08
One gap in stem wall	1.57	1.00
One gap in stem wall, low permeability fill	0.83	0.29
One gap in stem wall, low permeability fill, low radium fill	0.66	0.22
Restricted entry from stem wall interior to house	1.84	1.31

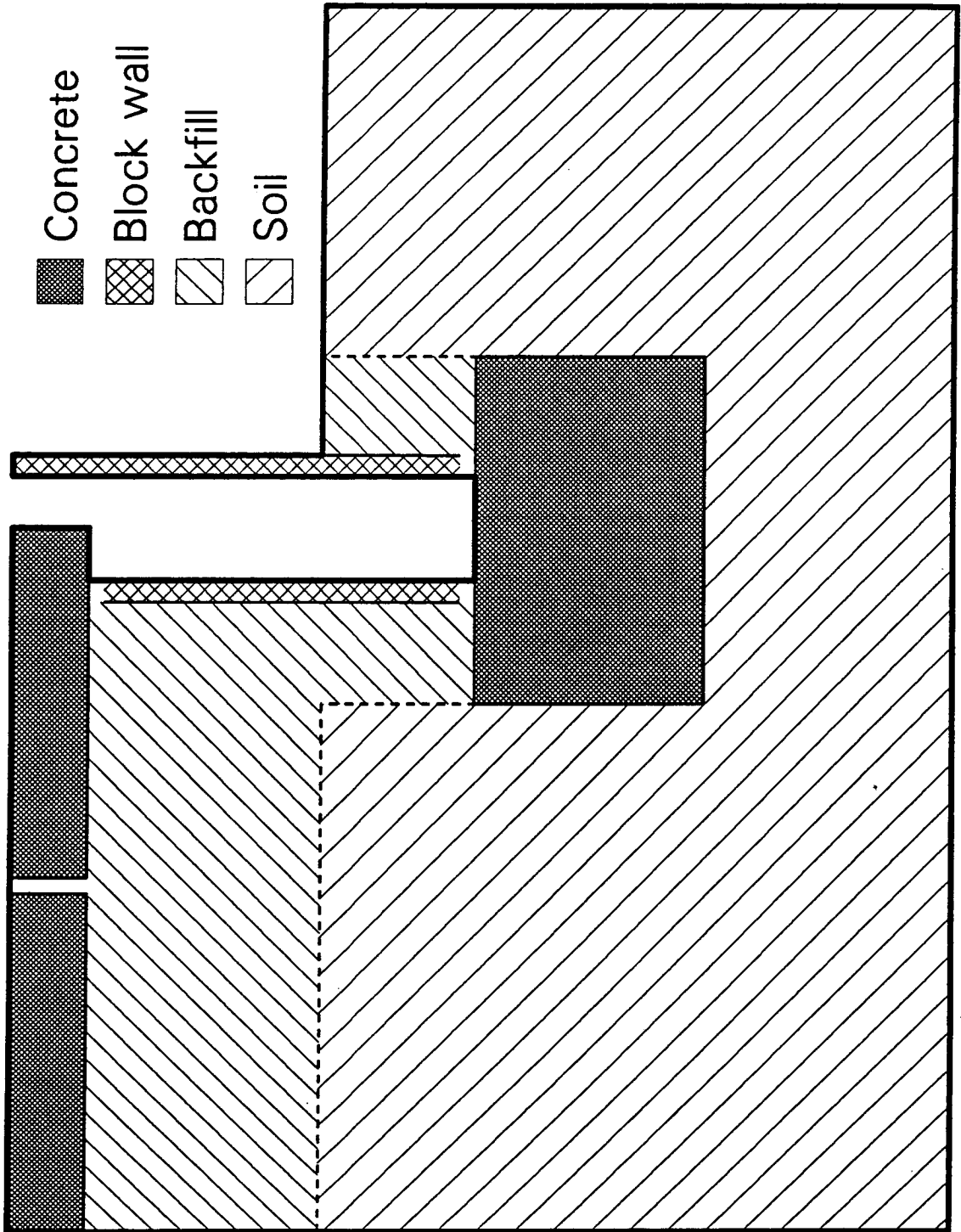
4. Summary of results for changes in fill and stem wall characteristics. The configurations listed in column 1 are described in more detail in the text.



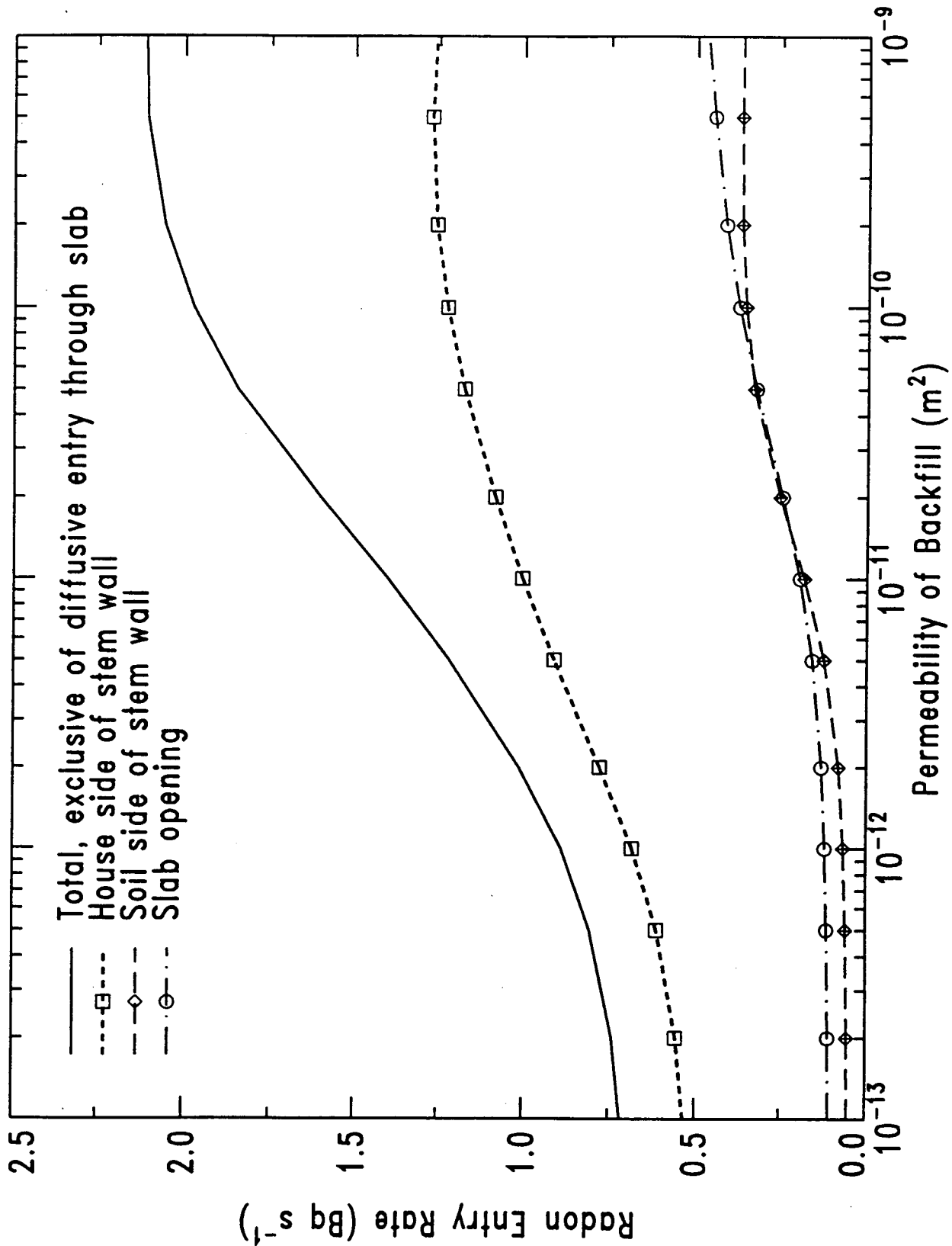
1. Detail of the vertical cross-section of the region modeled, showing the footer, stem wall, and part of the slab. The dimensions are those of the base configuration, as described in the text. The three gaps are shown exaggerated; their widths, in the base configuration, are each 0.003 m.



2. Vertical cross-section of the region of the model, with the boundaries for the present calculation shown as thick lines. The dimensions of the slab, backfill, soil, gaps, and openings are not to scale.



3. Vertical cross-section of the region of the model, with the boundaries for the mass-transport (radon concentration) calculation shown as thick lines. The dimensions of the slab, backfill, soil, gaps, and openings are not to scale.



4. Radon entry rates through three areas of the Florida substructure as functions of the backfill permeability. In order to increase the clarity of the figure, diffusive entry through the concrete slab has not been plotted; entry rates through the slab range from 0.51 to 0.55 Bq s⁻¹.

LAWRENCE BERKELEY LABORATORY
UNIVERSITY OF CALIFORNIA
TECHNICAL INFORMATION DEPARTMENT
BERKELEY, CALIFORNIA 94720